OPEN ACCESS

Original research

Modelling the cascade of biomarker changes in *GRN*-related frontotemporal dementia

Jessica L Panman ,[1,2] Vikram Venkatraghavan,[3] Emma L van der Ende ,[4] Rebecca M E Steketee,[3] Lize C Jiskoot ,[1] Jackie M Poos ,[1] Elise G P Dopper,[1] Lieke H H Meeter,[1] Laura Donker Kaat,[5] Serge A R B Rombouts,[2,6] Meike W Vernooij ,[3] Anneke J A Kievit,[5] Enrico Premi,[7] Maura Cosseddu,[7] Elisa Bonomi,[7] Jaume Olives,[8] Jonathan D Rohrer ,[9] Raquel Sánchez-Valle,[8,10] Barbara Borroni ,[7] Esther E Bron,[3] John C Van Swieten ,[1] Janne M Papma,[1] Stefan Klein,[3] GENFI consortium investigators

For numbered affiliations see end of article.

Correspondence to
Dr Jessica L Panman, Department of Neurology, Erasmus Medical Center, Rotterdam, Zuid-Holland, Netherlands; panman@essb.eur.nl

JLP and VV contributed equally.

Received 17 April 2020
Revised 19 October 2020
Accepted 24 November 2020

To cite: Panman JL, Venkatraghavan V, van der Ende EL, *et al*. *J Neurol Neurosurg Psychiatry* Epub ahead of print: [*please include* Day Month Year]. doi:10.1136/jnnp-2020-323541

ABSTRACT

Objective Progranulin-related frontotemporal dementia (FTD-*GRN*) is a fast progressive disease. Modelling the cascade of multimodal biomarker changes aids in understanding the aetiology of this disease and enables monitoring of individual mutation carriers. In this cross-sectional study, we estimated the temporal cascade of biomarker changes for FTD-*GRN*, in a data-driven way.

Methods We included 56 presymptomatic and 35 symptomatic *GRN* mutation carriers, and 35 healthy non-carriers. Selected biomarkers were neurofilament light chain (NfL), grey matter volume, white matter microstructure and cognitive domains. We used discriminative event-based modelling to infer the cascade of biomarker changes in FTD-*GRN* and estimated individual disease severity through cross-validation. We derived the biomarker cascades in non-fluent variant primary progressive aphasia (nfvPPA) and behavioural variant FTD (bvFTD) to understand the differences between these phenotypes.

Results Language functioning and NfL were the earliest abnormal biomarkers in FTD-*GRN*. White matter tracts were affected before grey matter volume, and the left hemisphere degenerated before the right. Based on individual disease severities, presymptomatic carriers could be delineated from symptomatic carriers with a sensitivity of 100% and specificity of 96.1%. The estimated disease severity strongly correlated with functional severity in nfvPPA, but not in bvFTD. In addition, the biomarker cascade in bvFTD showed more uncertainty than nfvPPA.

Conclusion Degeneration of axons and language deficits are indicated to be the earliest biomarkers in FTD-*GRN*, with bvFTD being more heterogeneous in disease progression than nfvPPA. Our data-driven model could help identify presymptomatic *GRN* mutation carriers at risk of conversion to the clinical stage.

INTRODUCTION

Mutations in the progranulin (*GRN*) gene on chromosome 17q21 are a major cause of autosomal dominant inherited frontotemporal dementia (FTD).[1 2] The majority of mutation carriers develops a behavioural variant FTD (bvFTD) phenotype,[3] and another significant proportion of patients present with non-fluent variant primary progressive aphasia (nfvPPA).[3 4] The age of symptom onset varies between 35 years and 90 years in *GRN* mutation carriers,[1 2] without clear associations with familial age of onset.[4] Brain changes in FTD-*GRN* patients can evolve symmetrically, or predominantly asymmetrically, in either the left or right hemisphere.[5 6]

Recent longitudinal studies have suggested that the time-window between emerging pathophysiological changes and the first clinical symptoms is short in *GRN* mutation carriers, and covers only 2–4 years.[7 8] During this period, the serum neurofilament light chain (NfL) level—a marker of axonal degeneration—increases twofold–threefold,[9 10] loss of grey and white matter emerges,[7 11] and cognitive functioning declines.[8] However, most of the biomarker studies in FTD-*GRN* have investigated one type of biomarker, that is, fluid, neuroimaging or cognition, leaving the temporal relations and ordering of these biomarkers unknown. These temporal relations could potentially provide novel insights into disease progression mechanisms in *GRN* mutation carriers. Moreover, because of the fast progression of pathophysiological changes, determining the earliest abnormal biomarker is crucial, as the optimal window of opportunity for treatment might be small.

Recently, novel data-driven methods for disease progression modelling have emerged, focusing on the cascade of biomarker changes.[12 13] Event-based models are a class of disease progression models that estimate the cascade of biomarker changes derived from cross-sectional data.[6 13 14] This is done without strong a priori assumptions regarding the relationship between different biomarkers. A promising novel method that estimates the cascade of biomarker change is discriminative event-based modelling (DEBM).[13 15] This model is robust to disease phenotypic heterogeneity in a cohort and can handle missing data.

In this study, we use DEBM to estimate the temporal cascade of biomarker changes in presymptomatic and symptomatic FTD-*GRN* mutation carriers, distinguishing between early and late

biomarkers. Furthermore, we determine phenotypic differences in patterns of biomarker changes in nfvPPA and bvFTD, to gain more insights into their distinct disease progression mechanisms.

METHODS

Sample and study procedures

Subjects were recruited prospectively from three European centres of the Genetic Frontotemporal dementia Initiative (GENFI): Rotterdam (the Netherlands), Brescia (Italy) and Barcelona (Spain). We collected cognitive and clinical data, MRI and serum samples from 126 participants. We included 35 symptomatic *GRN* mutation carriers (Rotterdam: n=11, Brescia: n=22, and Barcelona: n=2), 56 presymptomatic *GRN* mutation carriers (Rotterdam: n=33, Brescia: n=17, and Barcelona: n=6) and 35 cognitively healthy non-carriers (Rotterdam: n=34, Brescia: n=0, and Barcelona: n=1). Local clinical genetics departments performed DNA genotyping to confirm the presence of a *GRN* mutation. Non-carriers were first-degree family members of *GRN* patients without a mutation. Symptomatic mutation carriers were diagnosed based on the established clinical criteria for bvFTD[16] (n=17), nfvPPA[17] (n=16) or corticobasal syndrome[18] (n=2). Mutation carriers were defined as presymptomatic when clinical criteria were not fulfilled, that is, behavioural or cognitive symptoms were absent.[19] Clinical questionnaires were administered to the caregiver, spouse or a family member, that is, the Frontotemporal Lobar Degeneration Clinical Dementia Rating Scale Sum of Boxes (FTD-CDR-SOB),[20] the Neuropsychiatric Inventory (NPI)[21] and the Frontotemporal Dementia Rating Scale (FRS).[22] The study was carried out according to the Declaration of Helsinki, approved by the local medical ethics board at each site, and all participants provided written informed consent.

Biomarker collection and processing

Biomarker selection

For biomarker selection, we performed a literature search using Pubmed. We included studies that (1) performed research in presymptomatic *GRN* mutation carriers and (2) biomarker studies that examined biomarkers in blood or cerebrospinal fluid (CSF), neuroimaging biomarkers and cognition. We selected serum NfL,[9] Mini Mental State Examiation (MMSE), cognitive domains of attention and processing speed, executive functioning, language and social cognition[8 23]; left and right grey matter volumes of the insula, frontal lobe, parietal lobe and temporal lobe[7 11]; and left and right white matter tracts of the anterior thalamic radiation, superior longitudinal fasciculus, uncinate fasciculus and the forceps minor.[7 24] For detailed information about the literature review and subsequent biomarker selection, please see online supplemental appendix A.

Neurofilament light chain

Serum samples were obtained through venepunctures and analysed with single molecular assay technology, as described previously.[10] Samples were measured in a single laboratory, in duplicate, with an intra-assay coefficient of variation below 5%. Inter-assay variation between batches was below 8%. NfL concentrations were expressed in pg/mL.

MRI

Three-dimensional T1-weighted and diffusion tensor imaging were acquired with 3T MRI scanners across the three sites. MRI was missing in 25 participants due to unavailability (n=16) and insufficient quality due to motion artefacts (n=9). Availability of MRI and an overview of the scanning protocols are listed in online supplemental appendix A, Table A.1. Image processing was carried out in FMRIB Software Library (FSL),[25] using default pipelines for grey matter volumes and white matter tracts. For grey matter volumetric regions of interest (ROI), we used the Montreal Neurological Institute atlas,[26] and for the fractional anisotropy of white matter tracts, we used the Johns Hopkins University atlas.[27] Left and right regions and tracts were considered separately. Raw regional volumes and fractional anisotropy values were transformed to z-scores, based on the mean and SD from the non-carriers. A detailed description of processing and ROI calculation is reported in online supplemental appendix A.

Cognitive assessment

Cognitive data were collected from all participants in four cognitive domains, described in detail in online supplemental appendix A. Raw cognitive test scores were transformed to z-scores based on the mean and SD in non-carriers, and then combined into cognitive domain scores similar to previous studies.[8]

Confounding factors correction

All selected biomarkers were tested for normality (see online supplemental appendix A for details) and log-transformed in case of a skewed distribution. As most non-carriers originated from one centre, we used presymptomatic subjects for regressing out possible confounding effects using multiple linear regression, before continuing with event-based modelling. NfL levels were corrected for age and sex. Grey matter volumes and fractional anisotropy values were corrected for age, sex, total intracranial volume and MRI scanning protocol. Cognitive domain scores were corrected for confounding effects of age, sex and total years of education.

Temporal cascade of biomarker changes

The DEBM model introduced by Venkatraghavan *et al*[13 15] estimates the cascade of biomarker changes in a three-step process. For each biomarker, it first estimates the distributions of normal and pathological (or abnormal) values using Gaussian mixture modelling (GMM), and uses these to compute, for each subject, the probability that the biomarker is abnormal (explained in detail in online supplemental appendix B). The method then estimates the biomarker cascade independently for each subject based on the biomarker values present for that subject. The mean cascade is estimated such that the sum of the probabilistic Kendall's Tau distances is minimised between the mean cascade and all the subject-specific cascades. For subjects with missing biomarker values, only the corresponding subset of the biomarker cascade present in the subject-specific cascade is used to compute the probabilistic Kendall's Tau distance. Lastly, the severity of disease as a summary measure for each subject is computed by estimating the subject's progression along the resulting disease progression timeline. In this section, we describe the experiments we performed for estimating the cascade of biomarker changes for non-imaging biomarkers, as well as for neuroimaging and non-imaging biomarkers together.

DEBM model for non-imaging biomarkers

As imaging was missing in a lot of subjects (n=25), we first estimated the cascade of biomarker changes procedure with solely NfL and cognitive biomarkers. Since the non-carriers are healthy in this cohort, the normal Gaussians were fixed at the mean and SD of the biomarker values of the non-carriers. We used GMM only to estimate the abnormal Gaussian and the mixing

parameter for each biomarker. In order to estimate the positional variance in the estimated cascade, the entire dataset was randomly sampled using bootstrap sampling with 100 different random seeds, and the cascade of biomarker change was estimated for each of those randomly sampled datasets.[13 15]

DEBM model for neuroimaging and non-imaging biomarkers together

For the imaging biomarkers, we modified the GMM step in DEBM to make it better suited for the FTD-*GRN* population, known for its asymmetric pattern of atrophy.[5] Abnormal values of biomarkers that typically become abnormal late in the disease are usually under-represented in a specific patient population as compared with the early biomarkers. This could make the GMM of late biomarkers unstable, as previously reported.[15] Due to the asymmetrical atrophy patterns of FTD-*GRN*,[5 6] lateralised neuroimaging biomarkers that become abnormal early in the disease process may have a corresponding biomarker from the other hemisphere that remains stable until much later in the disease process. To exploit this, we assumed that the normal and abnormal Gaussians from the left and right hemispheric biomarkers (expressed as z-scores) are the same, and the biomarkers from both hemispheres only differ in their position along the disease progression timeline. With this assumption, we proposed a novel modification to the GMM optimisation called Siamese GMM, in which the biomarkers of the same region from left and right hemispheres are jointly optimised. The abnormal and normal Gaussians are shared between the left and right hemispheres, but the mixing parameters are independently estimated (see online supplemental appendix B for details). In this way, the numerical stability of GMM optimisation in the late neuroimaging biomarkers improved.

For non-imaging biomarkers, GMM was performed as described in the previous section. After GMM, further steps of DEBM modelling were carried out as usual, to estimate the complete cascade of neuroimaging and non-imaging biomarker changes in presymptomatic and symptomatic *GRN* mutation carriers. The positional variance in the estimated cascade was again estimated using bootstrap sampling with 100 different random seeds. For brevity, in the remainder of the paper, we refer to this model, which integrates neuroimaging and non-imaging biomarkers, as the multimodal DEBM.

Validation

To validate the DEBM models, we used 10-fold cross-validation. In each fold of the cross-validation, the DEBM model was built in the training set and the disease severity was estimated in the test set. We distinguished symptomatic mutation carriers from presymptomatic mutation carriers, and reported the corresponding sensitivity and specificity. Furthermore, in bvFTD and nfvPPA subjects, the estimated disease severity was correlated with years since symptom onset and FTD-CDR-SOB scores, using Pearson's correlation. Symptomatic carriers without imaging biomarkers were excluded for the validation of the multimodal DEBM but were included in the non-imaging DEBM.

Differential phenotype analysis

In order to examine the differences between bvFTD and nfvPPA variants of FTD-*GRN*, we built separate DEBM models. Presymptomatic subjects were excluded from this analysis as no phenotype information is available. The numbers of symptomatic subjects in each group (17 with bvFTD and 16 with nfvPPA) are too small to build complete DEBM models reliably. As a solution, we assumed that the biomarkers for the two phenotypes shared the same normal and abnormal biomarker distributions, and that they only differ in their position along the disease progression timeline. We hence optimised the GMM such that the normal and abnormal Gaussians were estimated without considering the phenotypes, whereas the mixing parameters were estimated separately for each phenotype. As before, we estimated the cascade of biomarker changes in the two phenotypes for non-imaging and multimodal (neuroimaging and non-imaging together) biomarkers.

RESULTS

Sample

A total of 126 subjects were included in this study. Availability and characteristics of the data are listed in table 1. Details on biomarker availability and characteristics can be found in online supplemental appendix, Tables A.2 and A.3. Symptomatic mutation carriers were older, had fewer years of education and had higher scores on the NPI and FTD-CDR-SOB, and lower scores on the FRS than both presymptomatic mutation carriers and non-carriers. There were no differences in demographic or clinical characteristics between presymptomatic mutation carriers and non-carriers.

Cascade of biomarker changes

Non-imaging and multimodal DEBM models

In figure 1A,B, we show the estimated mean cascade of biomarker changes and the uncertainty within the model for non-imaging and multimodal biomarkers. Language was the earliest biomarker to become abnormal, followed by NfL. It can be seen in figure 1B that left anterior thalamic radiation, left insula and bilateral uncinate fasciculi were the earliest imaging biomarkers. It can also be observed that imaging biomarkers from the left hemisphere became abnormal earlier than their right counterpart. GMM estimations with normal and abnormal Gaussian distributions are shown in figure 2, where the estimated Gaussians are seen to fit the observed histograms well. Figure 1C shows the positional variance of the cascade of multimodal biomarker changes obtained when GMM of the imaging biomarkers was done without using Siamese GMM. Generally, the positional variance was smaller with Siamese GMM than without.

Validation

Figure 3A,B shows the estimated disease severity when using non-imaging and multimodal biomarkers, respectively. It can be seen that estimated disease severity delineated the symptomatic subjects from the presymptomatic subjects. The sensitivity and specificity of this delineation were 1.0 and 0.982, respectively, while using non-imaging biomarkers, and 1.0 and 0.961, respectively, while using multimodal biomarkers.

Figure 4 shows the correlation of the estimated disease severity with years since symptom onset and FTD-CDR-SB for nfvPPA and bvFTD subjects, when using multimodal DEBM. It can be seen from figure 4 that estimated disease severity strongly correlated with years since symptom onset ($R=0.95$, $p=0.0003$) and the FTD-CDR-SB ($R=0.84$, $p=0.0189$) in nfvPPA patients. However, estimated disease severity correlated poorly with years since symptom onset ($R=0.22$, $p=0.6331$) and the FTD-CDR-SB ($R=0.28$, $p=0.5866$) in bvFTD patients. Online supplemental figure B.2 shows a similar plot when using non-imaging biomarkers, where estimated disease severity did

Table 1 Data availability and characteristics

	Symptomatic				
	Total	bvFTD	nfvPPA	Presymptomatic	Non-carriers
N					
Subjects (% female)	35* (60.0%)	17 (47.1%)	16 (75%)	56 (69.6%)	35 (54.4%)
Rotterdam	11	8	3	33	34
Brescia	22*	9	11	17	0
Barcelona	2	0	2	6	1
Data availability					
Serum NfL	91.7%	88.9%	93.8%	69.64%	91.67%
Cognitive assessment	91.7%	88.9%	93.8%	98.21%	91.67%
T1-weighted MRI	44.4%	38.9%	50.0%	96.4%	88.6%
DTI	50.0%	44.4%	56.3%	92.9%	91.4%
Sample characteristics					
Age (years)	62.57±6.72†	62.93±6.11‡	61.78±7.78§	51.52±11.42	55.15±12.55
Education (years)	10.61±4.59†	10.27±4.91‡	11.79±4.02	13.79±3.27	13.21±2.84
TIV (litres)	1.44±0.17	1.50±0.17	1.42±0.14	1.39±0.15	1.40±0.14
NPI	23.77±28.38†	28.90±30.64‡,¶	6.67±6.03¶	1.87±3.37	2.24±4.32
FRS	56.50±30.43†	48.86±29.91‡	67.20±30.96§	97.27±10.11	95.47±7.45
FTD-CDR-SOB	7.64±6.52†	9.68±7.47‡,¶	5.25±4.37§,¶	0.04±0.21	0.00±0.00
Disease duration (years)	2.45±2.01	2.37±1.92	2.48±2.29	N/A	N/A

*The two remaining patients presented with cortico-basal syndrome.
†Significant difference between symptomatic carriers and presymptomatic carriers as well as non-carriers.
‡Significant difference between bvFTD patients and presymptomatic patients as well as non-carriers.
§Significant difference between nfvPPA patients and presymptomatic patients as well as non-carriers.
¶Significant difference between bvFTD patients and nfvPPA patients.
bvFTD, behavioural variant frontotemporal dementia; DTI, diffusion tensor imaging; FRS, Frontotemporal Dementia Rating Scale; FTD-CDR-SOB, Frontotemporal Lobar Degeneration Clinical Dementia Rating Scale Sum of Boxes; mean±SD. GM, grey matter; NfL, neurofilament light chain; nfvPPA, non-fluent variant primary progressive aphasia; NPI, Neuropsychiatric Inventory; TIV, total intracranial volume.

not correlate with years since symptom onset and FTD-CDR-SB, neither for nfvPPA nor for bvFTD subjects.

Differential phenotype analysis

Figure 5 shows the multimodal biomarker cascade for nfvPPA and bvFTD phenotypes. nfvPPA patients showed language and NfL as first abnormal biomarkers followed by other cognitive domains. Left hemispheric imaging biomarkers became abnormal before right hemispheric imaging biomarkers, starting with the uncinated fasciculus (white matter integrity), insula and temporal lobe (grey matter volume). Only the left superior longitudinal fasciculus was estimated as late biomarker, even later then its right-sided counterpart.

Interestingly, in bvFTD patients, the biomarker ordering also indicated that language and NfL were the earliest abnormal biomarkers. In contrast to the nfvPPA, the left superior longitudinal fasciculus (white matter integrity) was estimated as the first abnormal imaging biomarker in bvFTD. However, the biomarker orderings in bvFTD were predominantly characterised by large uncertainty in the positioning of biomarkers in the disease timeline, with hardly any observable distinction between early and late biomarkers. Online supplemental figure B.3 presents the non-imaging biomarker cascade for the two phenotypes, showing that the uncertainty in the mean cascade in bvFTD is more than in nfvPPA.

DISCUSSION

In this study, we estimated the cascade of biomarker changes in FTD-*GRN*. We validated our model by delineating the symptomatic mutation carriers from the presymptomatic mutation carriers using the estimated disease severity. We demonstrated that language and NfL levels are the earliest biomarkers to become abnormal in the FTD-*GRN* spectrum. Other early biomarkers were the white matter microstructure of the thalamic

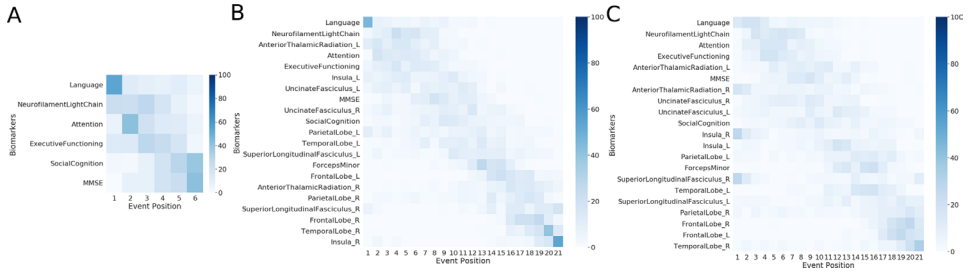

Figure 1 Cascade of biomarker changes in FTD-*GRN* along with the uncertainty associated with it. (A) Non-imaging biomarkers. (B) Multimodal biomarkers with Siamese GMM. (C) Multimodal biomarkers without Siamese GMM. The biomarkers are ordered based on the position in the estimated cascade. The colour map is based on the number of times a biomarker is at a position in 100 repetitions of bootstrapping. FTD-*GRN*, progranulin-related frontotemporal dementia; GMM, Gaussian mixture modelling.

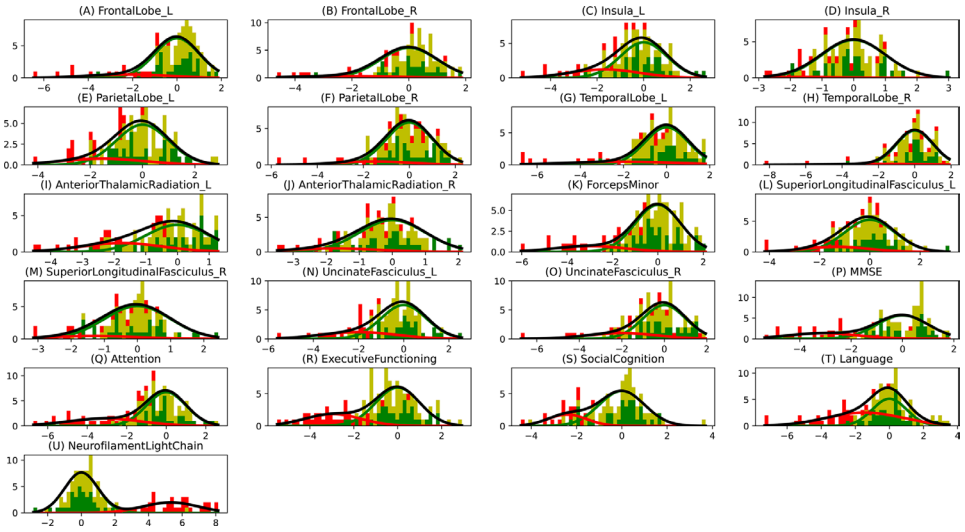

Figure 2 Gaussian mixture modelling (GMM) distributions. The histogram bins are divided in three colours, where the green part shows the proportion of non-carriers, the yellow part shows the proportion of presymptomatic carriers and the red part shows the proportion of symptomatic carriers. The Gaussians shown here are the ones that were estimated using GMM, where the green Gaussian is the normal one estimated using non-carriers and the red Gaussian is the abnormal one estimated using the carriers. The amplitudes of these Gaussians are based on the estimated mixing parameter. The grey curve shows the total estimated distribution, which is the summation of green and red Gaussians.

radiation and the cognitive domain of attention and mental processing speed.

Our findings support other studies that proposed NfL as an early biomarker for disease onset in FTD-*GRN*.[9 10] We demonstrated that the left anterior thalamic radiation also degenerated early. This is also supported by previous studies which suggested that white matter microstructure markers may correlate with changes in NfL.[9 28] Cognitive changes in attention, mental processing speed and executive functioning occurred relatively early in the estimated disease progression timeline. This corresponds well with the early white matter changes (ie, NfL and fractional anisotropy changes), as attention and processing speed are cognitive functions that highly depend on the integrity of axons and their myelin sheaths.[29 30] The early involvement of these biomarkers point towards axonal degeneration as one of the first pathological processes in *GRN* mutation carriers. However, it must be noted that the estimated cascade shows the sequence of biomarker events when they are detectably abnormal. One of the important factors that affects the detectability of biomarker abnormality in a cross-sectional dataset is the overlap between the normal and abnormal biomarker distributions. Therefore, the presented cross-sectional model cannot provide insight into the sequence of earliest (hardly detectable) changes in the carriers' biomarker levels. Figure 2 showed that the overlap in cognitive biomarkers was relatively smaller than the overlap in neuroimaging biomarkers, which could explain the relative early positioning of the cognitive biomarker events.

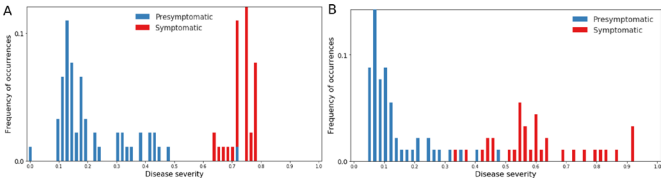

Figure 3 Frequency of occurrence of subjects with different disease severities, estimated using cross-validation. (A) Results using non-imaging biomarkers in discriminative event-based modelling (DEBM). (B) Results using multimodal biomarkers in DEBM.

With the differential phenotypic analysis, we estimated the biomarker cascade for nfvPPA and bvFTD patients. Strikingly, language functions deteriorated early in both nfvPPA and bvFTD. While not currently embedded in the clinical criteria for bvFTD,[16] our results demonstrate the importance of decreased language functions in both phenotypes. This is in line with multiple previous studies.[31–33] In addition, multiple determinants of the complex language network were also affected early, for example, the left insula and uncinate fasciculus.[34] While language deficits were estimated as the first detectable abnormal biomarker, the overlap with the second, the elevation in NfL levels, complicates distinguishing the timeline of these disease events. Furthermore, as depicted in figure 2, (subtle) language deficits were less specific for disease onset than NfL levels. However, the high sensitivity of the language biomarker in our study and the relative uncomplicated administration of language tests (compared with neuroimaging techniques, for example) offer potential for longitudinal research in the preclinical stage of FTD-*GRN*—ideally in combination with NfL levels.

For nfvPPA, NfL levels and other cognitive domains became abnormal in early disease stages, consistent with findings from previous studies.[9 10 35] In addition, we showed that left hemispheric tracts and regions were affected in nfvPPA patients before right regions, accordant with the previously reported strong involvement of the left hemisphere in primary progressive aphasia.[36 37] We showed that NfL levels and cognitive domains may be possible biomarkers for disease onset, while neuroimaging markers were highly correlated with clinical indicators of progression (years since onset, FTD-CDR-SOB).

For bvFTD, however, the biomarker cascade was characterised by large uncertainty, and the estimated disease severities did not correlate with actual years since onset or FTD-CDR-SOB. This uncertainty could indicate large neuroanatomical heterogeneities between bvFTD patients. Differences in neuroanatomical atrophy patterns have been associated with FTD-*GRN* patients before.[5 6] Here, we demonstrated that this anatomical heterogeneity is predominantly associated with the bvFTD phenotype, while nfvPPA patients showed a clear pattern of left hemispheric degeneration before the right hemisphere was affected.

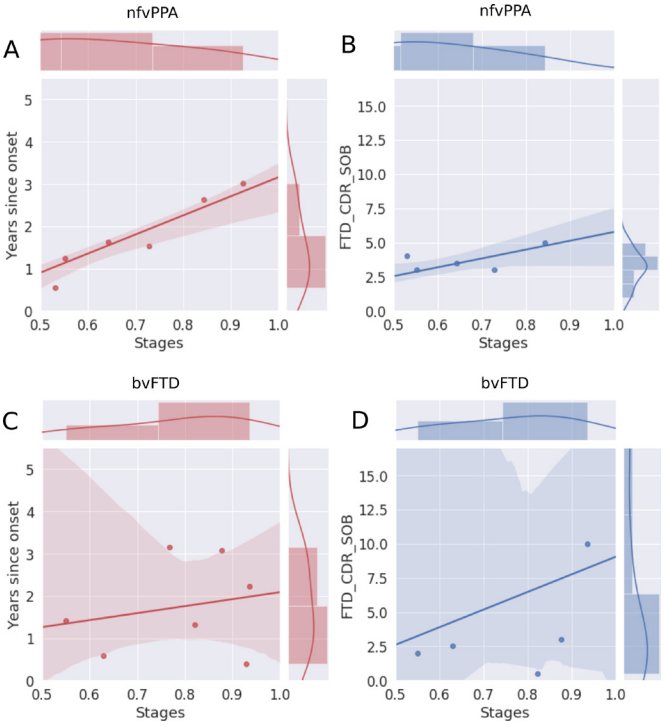

Figure 4 Correlation of disease severity (as estimated by multimodal DEBM using cross-validation) with years since onset and FTD-CDR-SOB. The 2D scatter plots in subfigures A and C show the correlations of disease severity with years since onset, for symptomatic nfvPPA and bvFTD subjects, respectively. The 2D scatter plot in subfigures B and D show the correlations of disease severity with FTD-CDR-SOB. The plot on top of each subfigure shows the probability density function of the disease stages. The plots on the right of subfigures A and C show the probability density functions of years since symptom onset. The plots on the right of subfigures B and D show the probability density function of FTD-CDR-SOB. 2D, two-dimensional; bvFTD, behavioural variant frontotemporal dementia; DEBM, discriminative event-based modelling; FTD-CDR-SOB, Frontotemporal Lobar Degeneration Clinical Dementia Rating Scale Sum of Boxes; nfvPPA, non-fluent variant primary progressive aphasia.

Furthermore, bvFTD patients present with cognitive symptoms such as impaired social conduct and executive function but can also have severe memory problems. In summary, within the group of bvFTD, spatial and temporal brain degeneration and cognitive changes are more heterogeneous than in the nfvPPA group.

From a methodological point of view, the strength of this paper lies in the introduction of the Siamese GMM approach in DEBM. We showed that Siamese GMM reduces the positional variance in neuroimaging biomarkers, most notably in the right insula, the right anterior thalamic radiation and the right superior longitudinal fasciculus. This is because GMM is known to be unstable in the presence of biomarkers with a large overlap between the normal and abnormal Gaussians.[13] This is often the case in biomarkers becoming abnormal late in the disease and having very few samples representative of the typical abnormal values expected in the disease. The joint GMM in the Siamese counterpart exploits the knowledge that FTD-*GRN* is generally an asymmetric brain disease, and uses the neuroimaging biomarkers that become abnormal early in the disease process to aid the GMM of its hemispheric counterpart that becomes abnormal far later in the disease process. Another strong point about the DEBM model is that it infers disease progression from cross-sectional data, which is more readily available than longitudinal data, especially in a rare disease as FTD-*GRN*.

From the clinical point of view, a major strength of our study is the large, well-defined cohort of presymptomatic and symptomatic *GRN* mutation carriers, and availability of multimodal (ie, fluid, imaging and cognitive) biomarkers. Although we did not have fluid-attenuated inversion recovery (FLAIR) or T2 imaging data available for the current study, it would be interesting to incorporate white matter lesions in a future version of the model, as a number of studies have indicated the presence of white matter lesions in FTD-*GRN* carriers.[38] Additionally, including functional neuroimaging, measures in future studies possibly provide new insights into the temporal biomarker sequence and underlying disease mechanism as well. Recent papers have addressed functional changes in FTD-*GRN*, showing thalamic-cortical hyperconnectivity in early preclinical stages[39] and presymptomatic abnormalities in neurophysiology.[40]

A minor limitation in our study is the difference in mean age between the non-carrier, presymptomatic and symptomatic mutation carrier groups. We adjusted for this in the analysis rather than matching the groups. It should be noted that the small sample size may have caused a large part of the uncertainty of our model, especially in the case of missing (neuroimaging) biomarkers. Our bvFTD and nfvPPA samples due to *GRN* mutations were relatively large compared with previous studies.[41] However, the DEBM model would improve substantially if the phenotypic samples were larger, as we could only include symptomatic subjects for the phenotypic analysis. Uncertainties in the estimation of the phenotypic biomarker cascades may be improved with upcoming longitudinal data, when some of the

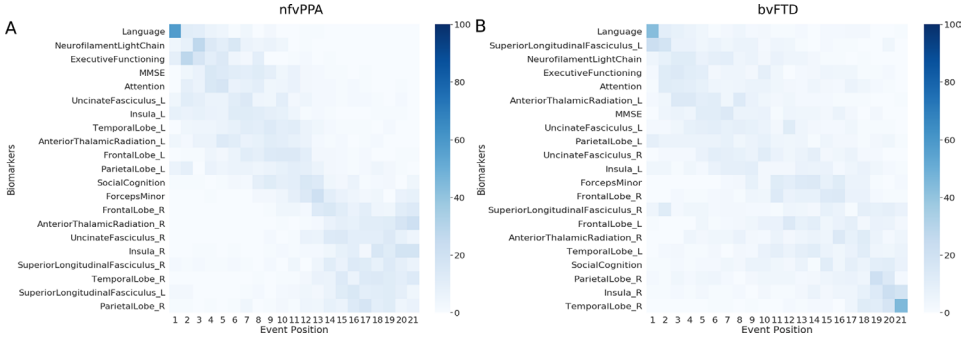

Figure 5 Cascade of multimodal biomarker changes in nfvPPA (A) and bvFTD (B) subjects along with the uncertainty associated with it. The biomarkers are ordered based on the position in the estimated cascade. The colour map is based on the number of times a biomarker is at a position in 100 repetitions of bootstrapping. bvFTD, behavioural variant frontotemporal dementia; nfvPPA, non-fluent variant primary progressive aphasia.

converted mutation carriers can be included in the phenotypic models.

In conclusion, with this DEBM study in the FTD-*GRN* spectrum, we were able to demonstrate that language functions and NfL levels are the earliest abnormal biomarkers, regardless of phenotype. However, bvFTD show more heterogeneity and uncertainty in disease progression, pointing towards more variability in biomarkers than nfvPPA. Our analyses suggest axonal degeneration and damage to the language network as the earliest biomarkers in *GRN* mutation carriers, which could potentially be used as endpoints in clinical trials for disease modifying treatments. Future efforts should be directed at confirmation and validation of these findings with longitudinal data. Validation of these results in an external cohort such as the Longitudinal Evaluation of Familial Frontotemporal Dementia Subjects (LEFFTDS)[42] could further aid in confirming these results and elucidate any ethnic variations in the disease progression timeline. We expect that DEBM modelling will benefit individual prediction of symptom onset in the future, and may optimise selection of eligible mutation carriers for clinical trials.

Author affiliations
[1]Department of Neurology, Erasmus Medical Center, Rotterdam, The Netherlands
[2]Department of Radiology, Leiden University Medical Center, Leiden, The Netherlands
[3]Department of Radiology and Nuclear Medicine, Erasmus Medical Center, Rotterdam, The Netherlands
[4]Department of Neurology, Erasmus MC, Rotterdam, The Netherlands
[5]Department of Clinical Genetics, Erasmus Medical Center, Rotterdam, The Netherlands
[6]Institute for Psychology, Leiden University, Leiden, The Netherlands
[7]Centre for Neurodegenerative Disorders, University of Brescia, Brescia, Italy
[8]Alzheimer's Disease and Other Cognitive Disorders Unit, Hospital Clínic de Barcelona, Barcelona, Spain
[9]Dementia Research Centre, UCL Institute of Neurology, London, UK
[10]Institut d'Investigacions Biomèdiques August Pi i Sunyer, Barcelona, Spain

Acknowledgements The authors wish to thank the patients and families for taking part in the FTD-RisC study and the Genetic Frontotemporal dementia Initiative cohort. Also, we thank Dr Ir Mark Bouts for the inspiration to commence this project.

Collaborators Genetic Frontotemporal dementia Initiative consortium: Sónia Afonso, Maria Rosario Almeida, Sarah Anderl-Straub, Christin Andersson, Anna Antonell, Silvana Archetti, Andrea Arighi, Mircea Balasa, Myriam Barandiaran, Nuria Bargalló, Robart Bartha, Benjamin Bender, Sandra Black, Chris Butler, Martina Bocchetta, Sergi Borrego-Ecija, Jose Bras, Rose Bruffaerts, Paola Caroppo, David Cash, Miguel Castelo-Branco, Rhian Convery, Thomas Cope, Adrian Danek, María de Arriba, Alexandre de Mendonça, Giuseppe Di Fede, Zigor Díaz, Simon Ducharme, Diana Duro, Chiara Fenoglio, Catarina B Ferreira, Elizabeth Finger, Toby Flanagan, Nick Fox, Morris Freedman, Giorgio Fumagalli, Alazne Gabilondo, Daniela Galimberti, Roberto Gasparotti, Serge Gauthier, Stefano Gazzina, Alexander Gerhard, Giorgio Giaccone, Ana Gorostidi, Caroline Graff, Caroline Greaves, Rita Guerreiro, Carolin Heller, Tobias Hoegen, Begoña Indakoetxea, Vesna Jelic, Hans-Otto Karnath Ron Keren Robert Laforce, Maria João Leitão, Johannes Levin, Albert Lladó, Sandra Loosli, Carolina Maruta, Mario Masellis, Simon Mead, Gabriel Miltenberger, Rick van Minkelenm Sara Mitchell, Katrina Moore, Fermin Moreno, Jennifer Nicholas, Linn Öijerstedt, Markus Otto, Sebastian Ourselin, Alessandro Padovani, Georgia Peakman, Yolande Pijnenburg, Cristina Polito, Sara Prioni, Catharina Prix, Rosa Rademakers, Veronica Redaelli, Tim Rittman, Ekaterina Rogaeva, Pedro Rosa-Neto, Giacomina Rossi, Martin Rosser, James Rowe, Isabel Santana, Beatriz Santiago, Elio Scarpini, Sonja Schönecker, Elisa Semler Rachelle Shafei, Christen Shoesmith, Matthis Synofzik, Miguel Tábuas-Pereira, Fabrizio Tagliavini, Carmela Tartaglia, Mikel Tainta, Ricardo Taipa, David Tang-Wai, David L Thomas, Hakan Thonberg, Carolyn Timberlake, Pietro Tiraboschi, Emily Todd, Philip Vandamme, Rik Vandenberghe, Mathieu Vandenbulcke, Michele Veldsman, Ana Verdelho, Jorge Villanua, Jason Warren, Carlo Wilkelone, Woollacott Elisabeth, Wlasich Henrik and Zetterberg Miren Zulaica.

Contributors JLP designed the study, collected and processed the data, performed analyses, and has written the manuscript. VV designed the model, performed analyses and has written the manuscript. EEB and SK have contributed to design of the model and writing of the manuscript. JCVS and JM Papma have contributed to the design of the study and writing of the manuscript. All other authors have collected data and contributed to writing of the manuscript.

Funding VV, MWV and SK have received funding from the European Union's Horizon 2020 research and innovation programme (grant agreement no. 666 992 (EuroPOND)). EEB was supported by the Hartstichting (PPP Allowance, 2018B011). The Dutch genetic frontotemporal dementia cohort is supported by Dioraphte Foundation (grant 09-02-00), the Association for frontotemporal Dementias Research Grant 2009, The Netherlands Organisation for Scientific Research (NWO; grant HCMI 056-13-018), ZonMw Memorabel (project nos. 733050103 and 733050813), the Bluefield project and JPND PreFrontAls consortium (project no. 733 051 042). LHHM was supported by Alzheimer Nederland project WE.09-2014-4. SAR was supported by NWO-Vici (grant 016-130-677). This study was partially funded by Fundació Marató de TV3, Spain (grant no. 20 143 810 to R Sanchez Valle). JDR is supported by an MRC Clinician Scientist Fellowship (MR/M008525/1) and has received funding from the NIHR Rare Disease Translational Research Collaboration (BRC149/NS/MH). This work was also supported by the MRC UK Genetic Frontotemporal dementia Initiative (GENFI; grant MR/M023664/1). The authors of this publication are members of GENFI and of the European Reference Network for Rare Neurological Diseases (project ID no. 739 510).

Competing interests RS-V received personal fees for participating in advisory meetings from Wave pharmaceuticals and Ionis.

Patient consent for publication Not required.

Ethics approval All patients and subjects included in this study provided written informed consent. The local ethics review boards at each site reviewed and approved the study.

Data availability statement Data are available upon reasonable request. The raw data of this project are part of Genetic Frontotemporal dementia Initiative and are not publicly available. Data can be accessed upon reasonable request to JCVS (j.c.vanswieten@erasmusmc.nl) and JDR (j.rohrer@ucl.ac.uk). The code for discriminative event-based modelling is available and can be downloaded from https://github.com/88vikram/pyebm/.

ORCID iDs
Jessica L Panman http://orcid.org/0000-0002-1126-6555
Emma L van der Ende http://orcid.org/0000-0003-2570-8796
Lize C Jiskoot http://orcid.org/0000-0002-1120-1858
Jackie M Poos http://orcid.org/0000-0001-8843-7247
Meike W Vernooij http://orcid.org/0000-0003-4658-2176
Jonathan D Rohrer http://orcid.org/0000-0002-6155-8417
Barbara Borroni http://orcid.org/0000-0001-9340-9814
John C Van Swieten http://orcid.org/0000-0001-6278-6844

REFERENCES

1 Seelaar H, Rohrer JD, Pijnenburg YAL, *et al*. Clinical, genetic and pathological heterogeneity of frontotemporal dementia: a review. *J Neurol Neurosurg Psychiatry* 2011;82:476–86.
2 van Swieten JC, Heutink P. Mutations in progranulin (GRN) within the spectrum of clinical and pathological phenotypes of frontotemporal dementia. *Lancet Neurol* 2008;7:965–74.
3 Mann DMA, Snowden JS. Frontotemporal lobar degeneration: pathogenesis, pathology and pathways to phenotype. *Brain Pathol* 2017;27:723–36.
4 Woollacott IOC, Rohrer JD. The clinical spectrum of sporadic and familial forms of frontotemporal dementia. *J Neurochem* 2016;138 Suppl 1: :6–31.
5 Chitramuthu BP, Bennett HPJ, Bateman A. Progranulin: a new avenue towards the understanding and treatment of neurodegenerative disease. *Brain* 2017;140:3081–104.
6 Young AL, Marinescu RV, Oxtoby NP, *et al*. Uncovering the heterogeneity and temporal complexity of neurodegenerative diseases with subtype and stage inference. *Nat Commun* 2018;9:4273.

7 Jiskoot LC, Panman JL, Meeter LH, *et al*. Longitudinal multimodal MRI as prognostic and diagnostic biomarker in presymptomatic familial frontotemporal dementia. *Brain* 2019;142:193–208.
8 Jiskoot LC, Panman JL, van Asseldonk L, *et al*. Longitudinal cognitive biomarkers predicting symptom onset in presymptomatic frontotemporal dementia. *J Neurol* 2018;265:1381–92.
9 Meeter LH, Dopper EG, Jiskoot LC, *et al*. Neurofilament light chain: a biomarker for genetic frontotemporal dementia. *Ann Clin Transl Neurol* 2016;3:623–36.
10 van der Ende EL, Meeter LH, Poos JM, *et al*. Serum neurofilament light chain in genetic frontotemporal dementia: a longitudinal, multicentre cohort study. *Lancet Neurol* 2019;18:1103–11.
11 Rohrer JD, Nicholas JM, Cash DM, *et al*. Presymptomatic cognitive and neuroanatomical changes in genetic frontotemporal dementia in the genetic frontotemporal dementia initiative (GENFI) study: a cross-sectional analysis. *Lancet Neurol* 2015;14:253–62.
12 Donohue MC, Jacqmin-Gadda H, Le Goff M, *et al*. Estimating long-term multivariate progression from short-term data. *Alzheimers Dement* 2014;10:S400–10.
13 Venkatraghavan V, Bron EE, Niessen WJ. A discriminative event based model for Alzheimer's disease progression modelling. *Information Processing in Medical Imaging* 2017:121–33.
14 Fonteijn HM, Modat M, Clarkson MJ, *et al*. An event-based model for disease progression and its application in familial Alzheimer's disease and Huntington's disease. *Neuroimage* 2012;60:1880–9.
15 Venkatraghavan V, Bron EE, Niessen WJ, *et al*. Disease progression timeline estimation for Alzheimer's disease using discriminative event based modeling. *Neuroimage* 2019;186:518–32.
16 Rascovsky K, Hodges JR, Knopman D, *et al*. Sensitivity of revised diagnostic criteria for the behavioural variant of frontotemporal dementia. *Brain* 2011;134:2456–77.
17 Gorno-Tempini ML, Hillis AE, Weintraub S, *et al*. Classification of primary progressive aphasia and its variants. *Neurology* 2011;76:1006–14.
18 Parmera JB, Rodriguez RD, Studart Neto A, *et al*. Corticobasal syndrome: a diagnostic conundrum. *Dement Neuropsychol* 2016;10:267–75.
19 Panman JL, Jiskoot LC, Bouts MJRJ, *et al*. Gray and white matter changes in presymptomatic genetic frontotemporal dementia: a longitudinal MRI study. *Neurobiol Aging* 2019;76:115–24.
20 Knopman DS, Kramer JH, Boeve BF, *et al*. Development of methodology for conducting clinical trials in frontotemporal lobar degeneration. *Brain* 2008;131:2957–68.
21 Cummings JL, Mega M, Gray K, *et al*. The neuropsychiatric inventory: comprehensive assessment of psychopathology in dementia. *Neurology* 1994;44:2308–14.
22 Mioshi E, Hsieh S, Savage S, *et al*. Clinical staging and disease progression in frontotemporal dementia. *Neurology* 2010;74:1591–7.
23 Barandiaran M, Moreno F, de Arriba M, *et al*. Longitudinal Neuropsychological Study of Presymptomatic c.709-1G>A Progranulin Mutation Carriers. *J Int Neuropsychol Soc* 2019;25:39–47.
24 Jiskoot LC, Bocchetta M, Nicholas JM, *et al*. Presymptomatic white matter integrity loss in familial frontotemporal dementia in the GENFI cohort: a cross-sectional diffusion tensor imaging study. *Ann Clin Transl Neurol* 2018;5:1025–36.
25 Jenkinson M, Beckmann CF, Behrens TEJ, *et al*. Fsl. *Neuroimage* 2012;62:782–90.
26 Collins DL, Holmes CJ, Peters TM, *et al*. Automatic 3-D model-based neuroanatomical segmentation. *Hum Brain Mapp* 1995;3:190–208.
27 Mori S, Wakana S, van Zijl PCM. *MRI atlas of Human White Matter*. Amsterdam, the Netherlands: Elsevier, 2005.
28 Menke RAL, Gray E, Lu C-H, *et al*. Csf neurofilament light chain reflects corticospinal tract degeneration in ALS. *Ann Clin Transl Neurol* 2015;2:748–55.
29 Tomimoto H. White matter integrity and cognitive dysfunction: radiological and neuropsychological correlations. *Geriatr Gerontol Int* 2015;15:3–9.
30 Hase Y, Horsburgh K, Ihara M, *et al*. White matter degeneration in vascular and other ageing-related dementias. *J Neurochem* 2018;144:617–33.
31 Hardy CJD, Buckley AH, Downey LE, *et al*. The language profile of behavioral variant frontotemporal dementia. *J Alzheimers Dis* 2016;50:359–71.
32 Ash S, Nevler N, Phillips J, *et al*. A longitudinal study of speech production in primary progressive aphasia and behavioral variant frontotemporal dementia. *Brain Lang* 2019;194:46–57.
33 Nevler N, Ash S, Jester C, *et al*. Automatic measurement of prosody in behavioral variant FTD. *Neurology* 2017;89:650–6.
34 Mesulam MM. Primary progressive aphasia and the left hemisphere language network. *Dement Neurocogn Disord* 2016;15:93–102.
35 Staffaroni AM, Ljubenkov PA, Kornak J, *et al*. Longitudinal multimodal imaging and clinical endpoints for frontotemporal dementia clinical trials. *Brain* 2019;142:443–59.
36 Grossman M. The non-fluent/agrammatic variant of primary progressive aphasia. *Lancet Neurol* 2012;11:545–55.
37 Rohrer JD, Rosen HJ. Neuroimaging in frontotemporal dementia. *Int Rev Psychiatry* 2013;25:221–9.
38 Sudre CH, Bocchetta M, Cash D, *et al*. White matter hyperintensities are seen only in *GRN* mutation carriers in the GENFI cohort. *Neuroimage Clin* 2017;15:171–80.
39 Lee SE, Sias AC, Kosik EL, *et al*. Thalamo-cortical network hyperconnectivity in preclinical progranulin mutation carriers. *Neuroimage Clin* 2019;22:101751.
40 Benussi A, Gazzina S, Premi E, *et al*. Clinical and biomarker changes in presymptomatic genetic frontotemporal dementia. *Neurobiol Aging* 2019;76:133–40.
41 Bonvicini C, Milanesi E, Pilotto A, *et al*. Understanding phenotype variability in frontotemporal lobar degeneration due to granulin mutation. *Neurobiol Aging* 2014;35): :1206–11.
42 Rosen HJ, Boeve BF, Boxer AL. Tracking disease progression in familial and sporadic frontotemporal lobar degeneration: recent findings from ARTFL and LEFFTDS. *Alzheimers Dement* 2020;16:71–8.

Appendix A. Biomarkers

Biomarker selection

For biomarker selection, we extensively searched for relevant literature about presymptomatic FTD-*GRN* in Pubmed. We reviewed all empirical studies that included at least a presymptomatic *GRN* mutation carrier group. Next, we determined which biomarkers were frequently reported as abnormal in previous empirical studies and included these biomarkers accordingly, restricted to fluid biomarkers, grey matter brain regions, white matter tracts, and cognition. The selected biomarkers were: serum NfL [1-3], MMSE [4-6], cognitive domains of language, attention and processing speed, executive functioning, and social cognition [5, 7-9]; left and right volumes of the insula, frontal lobe, parietal lobe and the temporal lobe [4, 6, 10-16] [17-19] [20, 21]; white matter tracts: left and right fractional anisotropy of anterior thalamic radiation, superior longitudinal fasciculus, uncinate fasciculus, and forceps minor [10, 17-19, 22, 23]. Although the *GRN* mutation affects plasma progranulin protein levels, these levels were not selected as biomarker, as research has shown that these remain stable in both the presymptomatic and symptomatic stage [6, 24].

MRI processing and ROI calculation

An overview of MRI acquisition parameters is presented in Appendix Table 1. The standard voxel-based morphometry pipeline from FSL [25-27] was used to process T1-weighted images. In brief, the brain was extracted from the images, and we carefully checked the brain extraction for missing brain tissue and areas of non-brain tissue, and adjusted the image accordingly. We corrected RF inhomogeneities by bias field correction with a Markov random field model and subsequently segmented the brain in grey matter, white matter, and cerebrospinal fluid images [28]. A study specific grey matter template was created in standard space using a balanced set of subjects, and all grey matter segmentations were registered to this template with non-linear registration,

and then corrected for any local expansion or contraction by modulation of the Jacobian warp field [26]. Last, an isotropic Gaussian kernel with a sigma of 3mm was applied for smoothing of the grey matter images. Total intracranial volume (TIV) was calculated as the sum of the volumes from grey matter, white matter and cerebrospinal fluid in standard space. The structures from the MNI-atlas were used as grey matter ROIs. We extracted volumetric measurements from the ROIs by registering the structural MNI-atlas [29] to the grey matter images in standard space, and multiplying the grey matter density of the ROI with the total volume of the ROI, resulting in the grey matter volume within the ROI. Left and right regions were considered separately.

Diffusion tensor images were corrected for motion artefacts and eddy currents by alignment to the b=0 image, and subsequently, the tensor was fitted at each voxel to create fractional anisotropy (FA) images. The FA images were processed with the tract-based spatial statistics (TBSS) pipeline as implemented in FSL [30]. Using non-linear registration, the images were aligned to the FMRIB58_FA template and then averaged into a mean FA image. The mean FA image was thresholded at 0.2 and thinned into a white matter skeleton. All individual FA images were projected onto this skeleton, resulting in skeletonized FA data for each participant. The probabilistic tracts from the Johns Hopkins University atlas [31] were applied as white matter ROIs to the skeleton mask, and the masked ROIs were used to extract FA values from the individual tracts. Left and right tracts were considered separately.

Table A.1. MRI acquisition protocols

	Rotterdam 1	**Rotterdam 2**	**Brescia**	**Barcelona**
N (s/p/nc)	3/22/24	5/9/6	7/17/0	1/6/1
Scanner	Philips Achieva 3T	Philips Achieva 3T	Siemens Skyra	Siemens Trio Tim
Head Coil	8 channel SENSE	32 channel SENSE	32 channel	64 channel
T1 weighted imaging				
TR	9.8 ms	6.8 ms	2000 ms	2000 ms
TE	4.6 ms	3.1 ms	2.9 ms	2.9 ms
FOV	224x168 mm	256x256 mm	282x282 mm	282x282 mm
Voxel size	0.88x0.88x1.2 mm	1.1mm^3	1.1 mm^3	1.1mm^3
Flip angle	8°	8°	8°	8°
Slices	140	207	208	208
Diffusion tensor imaging				
TR	8250 ms	7000 ms	7300 ms	7300 ms
TE	80 ms	69 ms	90 ms	90 ms
FOV	256x256 mm	240x240 mm	240x240 mm	240x240 mm
Voxel size	2x2x2mm	2.5x2.5x2.5mm	2.5x2.5x2.5mm	2.5x2.5x2.5mm
Slices	70	59	59	59
Directions	60	68	68	68
B-values	0/1000 s/mm^2	0/1000 s/mm^2	0/1000 s/mm^2	0/1000 s/mm^2

Numbers are subjects included after quality check. Abbreviations: s = symptomatic, p = presymptomatic, nc = non-carrier, TR = repetition time, TE = echo time, FOV = field of view.

Cognitive assessment

The following cognitive tests were performed, depending on the protocol from the local site. For language, the Boston Naming Task [32] and semantic fluency (animals) [33] were used. Tests concerning attention and processing speed were the Trail making test part A [34], Stroop part 1 and 2 [35], symbol substitution [36], letter digit substitution task [37], and forward digit span [36]. For executive functioning, we used Trail making test part B [34], Stroop task part 3 [35], phonological fluency [33] and digit span backwards [36]. Tests for social cognition were the Ekman faces test [38], emotion recognition from the mini social cognition and emotional assessment (MINI-SEA) [39], and Happé cartoon task [40]. Raw scores from tests in which a higher score indicates worse performance were reversed (i.e. Trail making test, Stroop). We transformed all raw test scores to z-scores, based on the mean and standard deviation of the non-carriers. Subsequently, cognitive domains were composed as the mean z-score of all available tests within that domain per individual, disregarding missing tests.

Table A.2. Availability and characteristics of cognitive data

	Symptomatic						**Presymptomatic**	
	Total (n=35)*		**bvFTD (n=17)**		**nfvPPA (n=16)**		**N=56**	
	N	*Mean ± SD*	*N*	*Mean ± SD*	*N*	*Mean ± SD*	*N*	*Mean ± SD*
MMSE	29	-3.07 ± 1.50	15	-3.26 ± 1.69	14	-2.87 ± 1.28	55	0.22 ± 1.01
Language	32	-2.86 ± 1.37	16	-2.69 ± 1.58	14	-3.00 ± 1.24	55	0.28 ± 1.09
Boston naming test	25	-1.97 ± 1.32	13	-1.75 ± 1.44	12	-2.21 ± 1.19	55	0.57 ± 1.37
Semantic fluency	31	-3.28 ± 1.38	15	-3.14 ± 1.57	14	-3.45 ± 1.30	55	0.00 ± 1.31
Attention, concentration and mental processing speed	33	-2.35 ± 1.17	16	-2.43 ± 1.32	15	-2.26 ± 1.12	55	-0.05 ± 0.75
TMT-A	32	-2.65 ± 1.62	16	-2.91 ± 1.63	14	-2.23 ± 1.66	55	-0.01 ± 0.92
Stroop card 1&2	17	-3.05 ± 2.18	10	-2.96 ± 2.20	7	-3.18 ± 2.32	55	0.14 ± 1.02
LDST	4	-2.06 ± 1.59	2	-2.09 ± 1.99	2	-2.03 ± 1.90	17	0.22 ± 0.70
Symbol substitution	17	-2.35 ± 1.41	7	-3.01 ± 1.13	10	-1.89 ± 1.45	22	0.00 ± 1.29
Digit span forward	31	-1.66 ± 1.05	15	-1.41 ± 1.29	14	-1.95 ± 0.74	55	-0.26 ± 0.95
Executive functioning	32	-2.33 ± 0.97	15	-2.23 ± 1.19	15	-2.37 ± 0.79	55	-0.03 ± 0.75
TMT-B	28	-2.63 ± 0.97	13	-2.50 ± 1.11	13	-2.69 ± 0.89	55	0.03 ± 0.79

Stroop card 3	14	-3.84 ± 2.29	8	-3.73 ± 2.50	6	-3.98 ± 2.20	55	-0.36 ± 1.05
Phonological fluency	29	-2.12 ± 0.95	14	-1.92 ± 1.02	15	-2.30 ± 0.87	55	0.30 ± 1.36
Digit span backwards	30	-1.65 ± 1.14	15	-1.61 ± 1.44	13	-1.61 ± 0.75	55	-0.08 ± 1.11
Social cognition	15	-1.87 ± 0.76	7	-2.15 ± 0.92	8	-1.62 ± 0.52	51	-0.10 ± 1.02
Ekman faces	3	-0.70 ± 0.60	2	-0.37 ± 0.18	1	-1.36 ± N/A	26	0.14 ± 0.89
Mini-SEA Emotion Recognition	10	-1.98 ± 0.83	3	-2.65 ± 1.13	7	-1.69 ± 0.52	22	-0.62 ± 0.98
HappeTOM	5	-2.07 ± 0.86	4	-2.32 ± 0.75	1	-1.05 ± N/A	28	0.42 ± 0.77
Happe non TOM	5	-1.65 ± 0.81	4	-1.81 ± 0.84	1	-1.03 ± N/A	28	0.34 ± 1.20

Abbreviations: bvFTD = behavioural variant frontotemporal dementia, nfvPPA = non-fluent variant primary progressive aphasia, MMSE = mini mental state examination, TMT = trail making test, LDST = letter digit substitution task, mini-SEA = mini social cognition and emotional assessment, TOM = theory of mind. Values are mean z-scores ± standard deviation based on non-carriers, uncorrected for confounding factors. * The two remaining participants presented with cortico-basal degeneration.

Biomarker statistics

Before modelling, we checked skewed distributions in the biomarkers with the following graphs and tests: histograms, q-q plots, skewness and kurtosis values (values between 2 and –2 indicate normality), Kolmogorov-Smirnov and Shapiro-Wilk's tests (values above 0.05 indicate normality). When three or more tests indicated skewness, the distributions were adjusted using log-transformations (log10), i.e. neurofilament light chain levels, MMSE, BNT, Trail Making Test, Stroop, facial emotion recognition. In the case of cognitive tests, log-transformation was performed before transforming raw scores to z-scores.

Biomarker characteristics and statistical differences between groups are presented in Table A.3. Symptomatic mutation carriers had higher NfL levels, lower grey matter volumes, impaired white matter microstructure, and worse cognitive functions than both presymptomatic mutation carriers and non-carriers in all selected biomarkers. Post-hoc analysis revealed that these differences in biomarkers were specifically driven by the bvFTD patients. For nfvPPA patients, we found higher NfL levels and worse cognitive performance than both presymptomatic mutation carriers and non-carriers. NfvPPA patients showed smaller grey matter volumes than both presymptomatic mutation carriers and non-carriers, especially in left-sided ROIs, and lower fractional anisotropy levels in the left anterior thalamic radiation, left uncinate fasciculus, and the forceps minor. The volume of the right frontal lobe was smaller in nfvPPA patients compared with presymptomatic mutation carriers. Furthermore, bvFTD patients had smaller volumes of the right frontal and temporal lobe than nfvPPA patients, and lower fractional anisotropy values in the forceps minor, left superior longitudinal fasciculus and right uncinate fasciculus. There were no differences in any of the selected biomarkers between presymptomatic mutation carriers and non-carriers.

Table A.3. Biomarker characteristics after correction for confounding factors

		Symptomatic			Presymptomatic
		Total	bvFTD	nfvPPA	
Neurofilament light chain		1.90 ± 0.25*	1.89 ± 0.23*	1.91 ± 0.28†	1.10 ± 0.22
GM volume	*Left frontal lobe*	-2.75 ± 1.8*	-3.42 ± 2.06*	-2.46 ± 1.40†	0.30 ± 0.65
	Right frontal lobe	-1.72 ± 1.79*	-2.76 ± 1.43*,‡	-0.93 ± 1.79§	0.30 ± 0.65
	Left insula	-2.32 ± 1.56*	-2.45 ± 1.79*	-2.35 ± 1.51†	-0.32 ± 0.95
	Right insula	-1.02 ± 1.13*	-1.47 ± 1.26*	-0.74 ± 0.98	-0.08 ± 0.84
	Left parietal lobe	-1.87 ± 1.11*	-2.18 ± 1.39*	-1.74 ± 0.84†	-0.03 ± 1.02
	Right parietal lobe	-1.19 ± 2.00*	-1.42 ± 2.08*	-0.89 ± 2.15	-0.06 ± 0.96
	Left temporal lobe	-2.97 ± 2.42*	-3.21 ± 2.59*	-2.98 ± 2.51†	-0.19 ± 0.96
	Right temporal lobe	-1.14 ± 2.66*	-2.22 ± 3.40*,‡	-0.12 ± 1.69	-0.08 ± 0.94
FA	*Left anterior thalmic radiation*	-2.28 ± 1.34*	-2.73 ± 1.60*	-1.77 ± 0.98†	-0.33 ± 0.95
	Right anterior thalamic radiation	-1.24 ± 1.23*	-1.78 ± 1.51*	-0.66 ± 0.66	-0.27 ± 0.77
	Forceps Minor	-3.00 ± 1.52*	-4.01 ± 1.52*,‡	-2.08 ± 0.96†	0.46 ± 0.93
	Left superior longitudinal fasciculus	-1.50 ± 1.39*	-2.42 ± 1.28*,‡	-0.61 ± 0.96	0.02 ± 0.88
	Right superior longitudinal fasciculus	-1.14 ± 1.12*	-1.47 ± 1.14*	-0.74 ± 1.06	-0.11 ± 0.60
	Left uncinated fasciculus	-2.63 ± 1.15*	-3.00 ± 1.43*	-2.29 ± 0.88†	-0.35 ± 0.86
	Right uncinate fasciculus	-1.92 ± 2.16*	-3.19 ± 2.07*,‡	-0.77 ± 1.74	-0.51 ± 1.12
MMSE		-2.71 ± 1.19*	-2.71 ± 1.28*	-2.71 ± 1.14†	0.06 ± 0.91
Attention and processing speed		-2.06 ± 1.09*	-2.11 ± 1.15*	-2.05 ± 1.12†	-0.22 ± 0.65

Executive functioning	-2.12 ± 0.88*	-2.00 ± 0.99*	-2.24 ± 0.82†	-0.14 ± 0.72
Language	-2.54 ± 1.23*	-2.35 ± 1.33*	-2.84 ± 1.17†	0.13 ± 0.97
Social cognition	-1.89 ± 0.64*	-2.13 ± 0.74*	-1.52 ± 0.42†	-0.19 ± 0.96

Abbreviations: bvFTD = behavioural variant frontotemporal dementia, nfvPPA = non-fluent variant primary progressive aphasia, GM volume = grey matter volume, FA = fractional anisotropy, MMSE = Mini Mental State Examination. Values are mean z-score (based on non-carriers) ± standard deviation, after correction for confounding factors of age, gender, MRI protocol, and years of education.

* Both the entire group of symptomatic mutation carriers and only bvFTD patients significantly differed from presymptomatic mutation carriers as well as non-carriers (*p<0.05*, Bonferroni corrected)

† Significant difference between nfvPPA patients and presymptomatic mutation carriers as well as non-carriers (*p<0.05*, Bonferroni corrected)

‡ Significant difference between bvFTD patients and nfvPPA patients (*p<0.05*, Bonferroni corrected)

¶ Significant difference between nfvPPA patients and presymptomatic mutation carriers (*p<0.05*, Bonferroni corrected)

References

1. Meeter, L.H., et al., *Neurofilament light chain: a biomarker for genetic frontotemporal dementia.* Ann Clin Transl Neurol, 2016. **3**(8): p. 623-36.
2. Rohrer, J.D., et al., *Serum neurofilament light chain protein is a measure of disease intensity in frontotemporal dementia.* Neurology, 2016. **87**(13): p. 1329-36.
3. van der Ende, E.L., et al., *Serum neurofilament light chain in genetic frontotemporal dementia: a longitudinal, multicentre cohort study.* Lancet Neurol, 2019. **18**(12): p. 1103-1111.
4. Rohrer, J.D., et al., *Presymptomatic cognitive and neuroanatomical changes in genetic frontotemporal dementia in the Genetic Frontotemporal dementia Initiative (GENFI) study: a cross-sectional analysis.* Lancet Neurol, 2015. **14**(3): p. 253-62.
5. Jiskoot, L.C., et al., *Longitudinal cognitive biomarkers predicting symptom onset in presymptomatic frontotemporal dementia.* J Neurol, 2018.
6. Benussi, A., et al., *Clinical and biomarker changes in presymptomatic genetic frontotemporal dementia.* Neurobiol Aging, 2019. **76**: p. 133-140.
7. Barandiaran, M., et al., *Neuropsychological features of asymptomatic c.709-1G>A progranulin mutation carriers.* J Int Neuropsychol Soc, 2012. **18**(6): p. 1086-90.
8. Barandiaran, M., et al., *Longitudinal Neuropsychological Study of Presymptomatic c.709-1G>A Progranulin Mutation Carriers.* J Int Neuropsychol Soc, 2019. **25**(1): p. 39-47.
9. Jiskoot, L.C., et al., *Presymptomatic cognitive decline in familial frontotemporal dementia: A longitudinal study.* Neurology, 2016. **87**(4): p. 384-91.
10. Borroni, B., et al., *Brain magnetic resonance imaging structural changes in a pedigree of asymptomatic progranulin mutation carriers.* Rejuvenation Res, 2008. **11**(3): p. 585-95.
11. Cash, D.M., et al., *Patterns of gray matter atrophy in genetic frontotemporal dementia: results from the GENFI study.* Neurobiol Aging, 2017. **62**: p. 191-196.

12. Premi, E., et al., *Subcortical and Deep Cortical Atrophy in Frontotemporal Dementia due to Granulin Mutations.* Dement Geriatr Cogn Dis Extra, 2014. **4**(1): p. 95-102.
13. Young, A.L., et al., *Uncovering the heterogeneity and temporal complexity of neurodegenerative diseases with Subtype and Stage Inference.* Nat Commun, 2018. **9**(1): p. 4273.
14. Jacova, C., et al., *Anterior brain glucose hypometabolism predates dementia in progranulin mutation carriers.* Neurology, 2013. **81**(15): p. 1322-31.
15. Popuri, K., et al., *Gray matter changes in asymptomatic C9orf72 and GRN mutation carriers.* Neuroimage Clin, 2018. **18**: p. 591-598.
16. Moreno, F., et al., *Distinctive age-related temporal cortical thinning in asymptomatic granulin gene mutation carriers.* Neurobiol Aging, 2013. **34**(5): p. 1462-8.
17. Dopper, E.G., et al., *Structural and functional brain connectivity in presymptomatic familial frontotemporal dementia.* Neurology, 2014. **83**(2): p. e19-26.
18. Jiskoot, L.C., et al., *Longitudinal multimodal MRI as prognostic and diagnostic biomarker in presymptomatic familial frontotemporal dementia.* Brain, 2019. **142**(1): p. 193-208.
19. Panman, J.L., et al., *Gray and white matter changes in presymptomatic genetic frontotemporal dementia: a longitudinal MRI study.* Neurobiol Aging, 2019. **76**: p. 115-124.
20. Pievani, M., et al., *Pattern of structural and functional brain abnormalities in asymptomatic granulin mutation carriers.* Alzheimers Dement, 2014. **10**(5 Suppl): p. S354-S363 e1.
21. Caroppo, P., et al., *Lateral Temporal Lobe: An Early Imaging Marker of the Presymptomatic GRN Disease?* J Alzheimers Dis, 2015. **47**(3): p. 751-9.
22. Jiskoot, L.C., et al., *Presymptomatic white matter integrity loss in familial frontotemporal dementia in the GENFI cohort: A cross-sectional diffusion tensor imaging study.* Ann Clin Transl Neurol, 2018. **5**(9): p. 1025-1036.

23. Olm, C.A., et al., *Longitudinal structural gray matter and white matter MRI changes in presymptomatic progranulin mutation carriers.* Neuroimage Clin, 2018. **19**: p. 497-506.
24. Meeter, L.H., et al., *Progranulin Levels in Plasma and Cerebrospinal Fluid in Granulin Mutation Carriers.* Dement Geriatr Cogn Dis Extra, 2016. **6**(2): p. 330-340.
25. Douaud, G., et al., *Anatomically related grey and white matter abnormalities in adolescent-onset schizophrenia.* Brain, 2007. **130**(Pt 9): p. 2375-86.
26. Jenkinson, M., et al., *Fsl.* Neuroimage, 2012. **62**(2): p. 782-90.
27. Smith, S.M., et al., *Advances in functional and structural MR image analysis and implementation as FSL.* Neuroimage, 2004. **23 Suppl 1**: p. S208-19.
28. Zhang, Y., M. Brady, and S. Smith, *Segmentation of brain MR images through a hidden Markov random field model and the expectation-maximization algorithm.* IEEE Trans Med Imaging, 2001. **20**(1): p. 45-57.
29. Collins, D.L., Holmes, C.J., Peters, T.M., Evans, A.C., *Automated 3-D model-based neuroanatomical segmentation.* Human Brain Mapping, 1995. **3**(3): p. 190-208.
30. Smith, S.M., et al., *Tract-based spatial statistics: voxelwise analysis of multi-subject diffusion data.* Neuroimage, 2006. **31**(4): p. 1487-505.
31. Mori, S., Wakana, S, van Zijl, P.C.M, Nagae-Poetscher, L.M., *MRI atlas of Human White Matter*. 2005, Amsterdam, the Netherlands: Elsevier.
32. Kaplan, E., Goodglass, H., Weintraub, S., *Boston Naming Test*. 1983, Philadelphia: Lea & Febiger.
33. Thurstone, L.L., Thurstone, T.G., *Primary Mental Abilities*. 1962, Chicago: University of Chicago Press.
34. battery, A.i.t., *Manual of directions and scoring*. 1944, Washington, DC: War Department, Adjunct General's Office.
35. Stroop, J., *Studies of interference in serial verbal reaction.* Journal of Experimental Psychology, 1935. **18**: p. 643-662.

36. Wechsler, D., *WAIS-III Technische Handleiding*. 2005, Amsterdam: Harcourt Test Publishers.

37. Jolles, J., Houx, P.K., van Boxtel, M.P.J., Ponds R.W.H.M., *Maastricht aging study: Determinants of cognitive aging*. 1995, Maastricht: Neuropsych Publishers.

38. Ekman, P., Friesen, W.V., *Pictures of facial affect* 1976, Palo Alto, CA: Consulting Psychological Press.

39. Funkiewiez, A., et al., *The SEA (Social cognition and Emotional Assessment): a clinical neuropsychological tool for early diagnosis of frontal variant of frontotemporal lobar degeneration.* Neuropsychology, 2012. **26**(1): p. 81-90.

40. Happe, F., H. Brownell, and E. Winner, *Acquired 'theory of mind' impairments following stroke.* Cognition, 1999. **70**(3): p. 211-40.

APPENDIX B – DISCRIMINATIVE EVENT BASED MODELLING

DEBM: Gaussian mixture modelling

DEBM uses Gaussian mixture modelling to transform biomarker values to posterior probabilities of them being abnormal. This is done by assuming the probability density functions of normal and abnormal values are represented by Gaussians $N(\mu_{\sim E}, \sigma_{\sim E})$and $N(\mu_E, \sigma_E)$ respectively, where the occurrence of the biomarker abnormality event is denoted by E and the absence of such an event is denoted by $\sim E$.

Gaussian mixture modelling is an optimisation task to estimate these normal and abnormal Gaussians as well as the mixing parameter based on maximum log-likelihood, where the log-likelihood for biomarker B is computed as the summation over all *GRN* mutation carriers in the dataset as follows:

$$L_B = \sum_{\forall j \in Carriers} \log f(B_j)$$

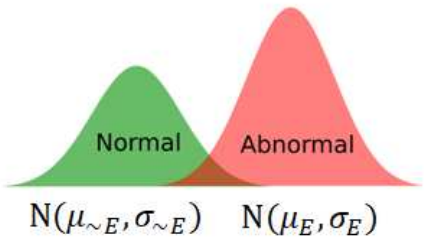

Figure B.1: Illustrations of the Gaussian probability density functions for normal and abnormal values of biomarker B

Here, the likelihood $f(B)$ is computed as follows:

$$f(B) = \theta_{\sim E} p(B|\mu_{\sim E}, \sigma_{\sim E}) + \theta_E p(B|\mu_E, \sigma_E),$$

Where $\theta_{\sim E} + \theta_E = 1$, and the mixing parameters $\theta_{\sim E}$ and θ_E show the relative proportions of the two Gaussians in the dataset. The abnormal Gaussian is initialized using the mean and standard deviation of the symptomatic subjects, while the normal Gaussian is initialized using the non-carriers. Since non-carriers are healthy controls, we fix $\mu_{\sim E}$ and $\sigma_{\sim E}$ to their initialized values and only optimize the remaining parameters in the Gaussian mixture model. The mixing parameter and the Gaussian parameters are optimized alternately until convergence as detailed previously,[1].

For imaging-biomarkers with left and right counter parts, we propose a novel modification to the Gaussian mixture model optimization called Siamese Gaussian mixture model (Siamese GMM). We propose to jointly optimize the parameters of these biomarkers, by taking advantage of symmetry in the brain. The log-likelihood for the joint optimization for the imaging biomarkers I^L and $I^R$is given below:

$$L_I = \sum_{\forall j \in Carriers} \log f\left(I^L{}_j\right) + \log f\left(I^R{}_j\right)$$

where $f\left(I^L{}_j\right)$ and $f\left(I^R{}_j\right)$ are expressed mathematically as:

$$f\left(I^L{}_j\right) = \theta^L_{\sim E} p\left(I^L{}_j \middle| \mu_{\sim E}, \sigma_{\sim E}\right) + \theta^L_E p\left(I^L{}_j \middle| \mu_E, \sigma_E\right)$$

$$f\left(I^R{}_j\right) = \theta^R_{\sim E} p\left(I^R{}_j \middle| \mu_{\sim E}, \sigma_{\sim E}\right) + \theta^R_E p\left(I^R{}_j \middle| \mu_E, \sigma_E\right)$$

$\theta^L_{\sim E} + \theta^L_E = 1$ and $\theta^R_{\sim E} + \theta^R_E = 1$. The mixing parameters $(\theta^L_{\sim E}, \theta^L_E, \theta^R_{\sim E}, \theta^R_E)$ and the abnormal Gaussian parameters $(\mu_E,\ \sigma_E)$ are again optimized alternately until convergence,[1]. This joint optimization of the left and right counter parts by sharing the normal and abnormal Gaussians reduces the number of parameters to be optimized, and thus improves the robustness. In case of asymmetrical atrophy patterns, where one of the biomarkers is stronger than the other, the joint optimization also helps in making the GMM more stable for the weaker biomarker.

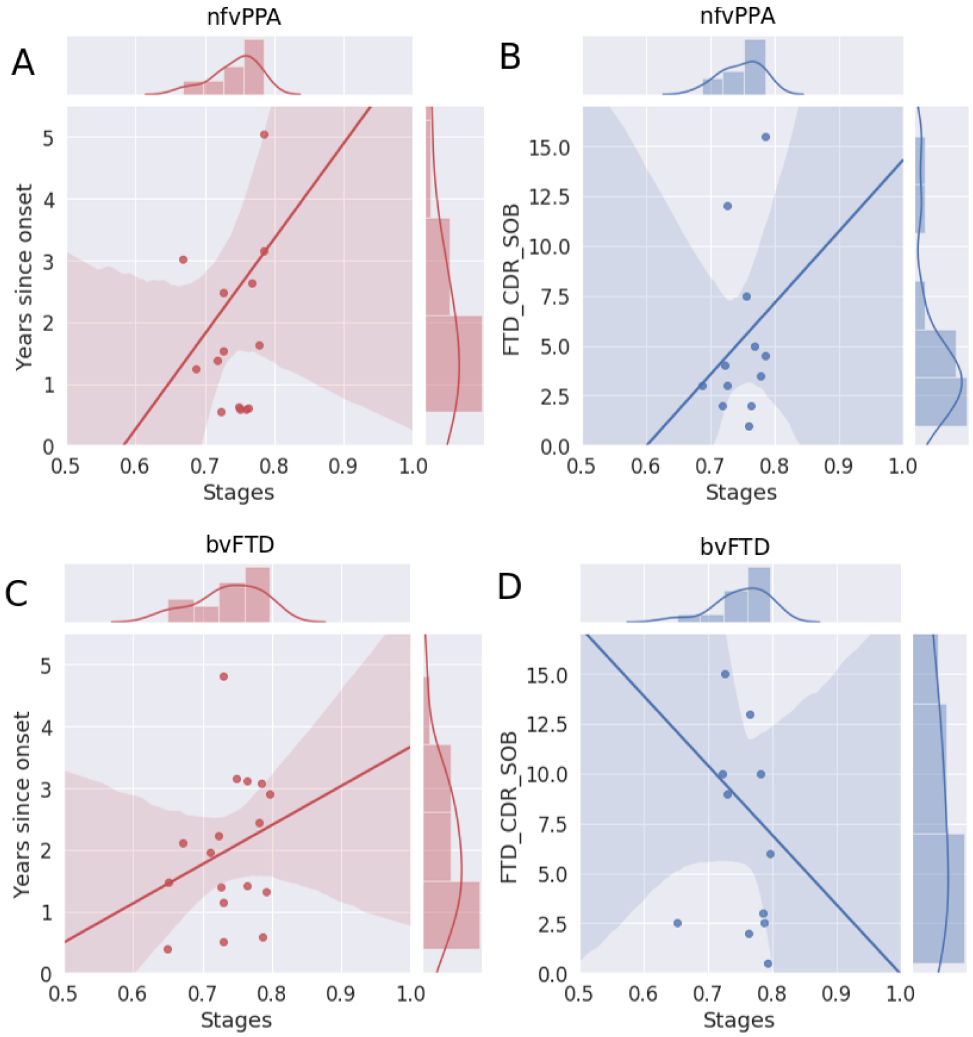

Figure B.2. Correlation of disease severity (as estimated by non-imaging DEBM using cross-validation) with years since onset and FTD-CDR-SOB. The 2D scatter plots in figures A and C show the correlations of disease severity with years since onset, for symptomatic nfvPPA and bvFTD subjects respectively. The 2D scatter plot in figures B and D show the correlations of disease severity with FTD-CDR-SOB. The plot on top of each subfigure shows the probability density function of the disease stages. The plots on the right of figures A and C show the probability density functions of years since symptom onset. The plots on the right of figures B and D show the probability density function of FTD-CDR-SOB.

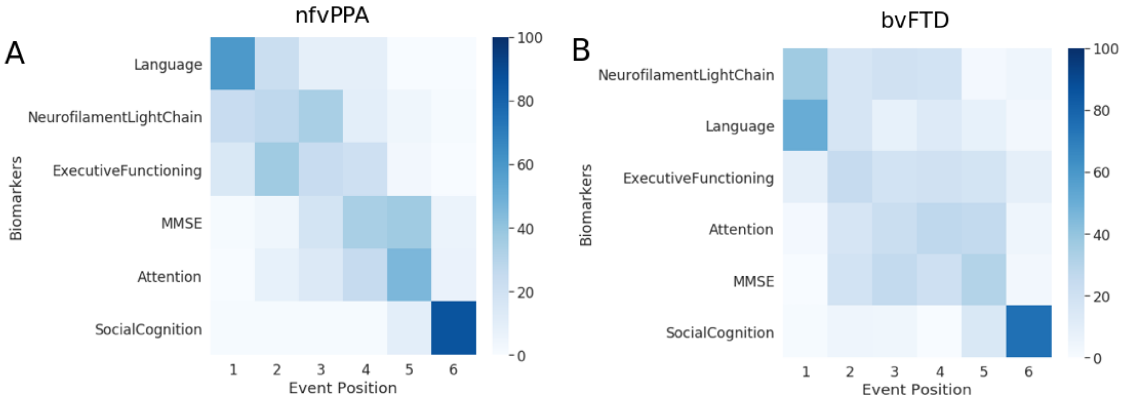

Figure B.3. Cascade of non-imaging biomarker changes in nfvPPA (A) and bvFTD (B) subjects along with the uncertainty associated with it. The biomarkers are ordered based on the position in the estimated cascade. The color-map is based on the number of times a biomarker is at a position in 100 repetitions of bootstrapping.

References

1. Venkatraghavan, V., Bron, E.E., Wiessen, W.J., et al., *Disease progression timeline estimation for Alzheimer's disease using discriminative event based modeling.* Neuroimage, 2019. **186**: p. 518-532.

Appendix C – GENFI consortium members

Author	Affiliation
Sónia Afonso	Instituto Ciencias Nucleares Aplicadas a Saude, Universidade de Coimbra, Coimbra, Portugal
Maria Rosario Almeida	Faculty of Medicine, University of Coimbra, Coimbra, Portugal
Sarah Anderl-Straub	Department of Neurology, University of Ulm, Ulm, Germany
Christin Andersson	Department of Clinical Neuroscience, Karolinska Institutet, Stockholm, Sweden
Anna Antonell	Alzheimer's disease and Other Cognitive Disorders Unit, Neurology Service, Hospital Clínic, Barcelona, Spain
Silvana Archetti	Biotechnology Laboratory, Department of Diagnostics, Spedali Civili Hospital, Brescia, Italy
Andrea Arighi	Fondazione IRCCS Ca' Granda Ospedale Maggiore Policlinico, Neurodegenerative Diseases Unit, Milan, Italy; University of Milan, Centro Dino Ferrari, Milan, Italy
Mircea Balasa	Alzheimer's disease and Other Cognitive Disorders Unit, Neurology Service, Hospital Clínic, Barcelona, Spain
Myriam Barandiaran	Cognitive Disorders Unit, Department of Neurology, Donostia University Hospital, San Sebastian, Gipuzkoa, Spain; Neuroscience Area, Biodonostia Health Research Insitute, San Sebastian, Gipuzkoa, Spain
Nuria Bargalló	Imaging Diagnostic Center, Hospital Clínic, Barcelona, Spain
Robart Bartha	Department of Medical Biophysics, The University of Western Ontario, London, Ontario, Canada; Centre for Functional and Metabolic Mapping, Robarts Research Institute, The University of Western Ontario, London, Ontario, Canada
Benjamin Bender	Department of Diagnostic and Interventional Neuroradiology, University of Tübingen, Tübingen, Germany
Sandra Black	Sunnybrook Health Sciences Centre, Sunnybrook Research Institute, University of Toronto, Toronto, Canada
Chris Butler	Department of Clinical Neurology, University of Oxford, Oxford, UK
Martina Bocchetta	Dementia Research Centre, Department of Neurodegenerative Disease, UCL Institute of Neurology, Queen Square, London, UK
Sergi Borrego-Ecija	Alzheimer's disease and Other Cognitive Disorders Unit, Neurology Service, Hospital Clínic, Barcelona, Spain
Jose Bras	Dementia Research Institute, Department of Neurodegenerative Disease, UCL Institute of Neurology, Queen Square, London, UK
Rose Bruffaerts	Laboratory for Cognitive Neurology, Department of Neurosciences, KU Leuven, Leuven, Belgium
Paola Caroppo	Fondazione IRCCS Istituto Neurologico Carlo Besta, Milano, Italy
David Cash	Dementia Research Centre, Department of Neurodegenerative Disease, UCL Institute of Neurology, Queen Square, London, UK
Miguel Castelo-Branco	Faculty of Medicine, University of Coimbra, Coimbra, Portugal

Rhian Convery	Dementia Research Centre, Department of Neurodegenerative Disease, UCL Institute of Neurology, Queen Square, London, UK
Thomas Cope	Department of Clinical Neuriscience, University of Cambridge, Cambridge, UK
Adrian Danek	Neurologische Klinik und Poliklinik, Ludwig-Maximilians-Universität, Munich, German Center for Neurodegenerative Diseases (DZNE), Munich, Germany
María de Arriba	Neuroscience Area, Biodonostia Health Research Insitute, San Sebastian, Gipuzkoa, Spain
Alexandre de Mendonça	Faculty of Medicine, University of Lisbon, Lisbon, Portugal
Giuseppe Di Fede	Fondazione IRCCS Istituto Neurologico Carlo Besta, Milano, Italy
Zigor Díaz	CITA Alzheimer, San Sebastian, Gipuzkoa, Spain
Simon Ducharme	Department of Psychiatry, McGill University Health Centre, McGill University, Montreal, Québec, Canada
Diana Duro	Faculty of Medicine, University of Coimbra, Coimbra, Portugal
Chiara Fenoglio	Fondazione IRCCS Ca' Granda Ospedale Maggiore Policlinico, Neurodegenerative Diseases Unit, Milan, Italy; University of Milan, Centro Dino Ferrari, Milan, Italy
Catarina B. Ferreira	Laboratory of Neurosciences, Institute of Molecular Medicine, Faculty of Medicine, University of Lisbon, Lisbon, Portugal
Elizabeth Finger	Department of Clinical Neurological Sciences, University of Western Ontario, London, ON, Canada
Toby Flanagan	Faculty of Biology, Medicine and Health, Division of Neuroscience and Experimental Psychology, University of Manchester, Manchester, UK
Nick Fox	Dementia Research Centre, Department of Neurodegenerative Disease, UCL Institute of Neurology, Queen Square, London, UK
Morris Freedman	Baycrest Health Sciences, Rotman Research Institute, University of Toronto, Toronto, Canada
Giorgio Fumagalli	Fondazione IRCCS Ca' Granda Ospedale Maggiore Policlinico, Neurodegenerative Diseases Unit, Milan, Italy; University of Milan, Centro Dino Ferrari, Milan, Italy; Department of Neurosciences, Psychology, Drug Research and Child Health (NEUROFARBA), University of Florence, Florence, Italy
Alazne Gabilondo	Neuroscience Area, Biodonostia Health Research Insitute, San Sebastian, Gipuzkoa, Spain
Daniela Galimberti	Fondazione IRCCS Ca' Granda Ospedale Maggiore Policlinico, Neurodegenerative Diseases Unit, Milan, Italy
Roberto Gasparotti	Neuroradiology Unit, University of Brescia, Brescia, Italy
Serge Gauthier	Alzheimer Disease Research Unit, McGill Centre for Studies in Aging, Department of Neurology & Neurosurgery, McGill University, Montreal, Québec, Canada
Stefano Gazzina	Centre for Neurodegenerative Disorders, Neurology Unit, Department of Clinical and Experimental Sciences, University of Brescia, Brescia, Italy
Alexander Gerhard	Institute of Brain, Behaviour and Mental Health, The University of Manchester, Withington, Manchester, UK
Giorgio Giaccone	Fondazione IRCCS Istituto Neurologico Carlo Besta, Milano, Italy

Ana Gorostidi	Neuroscience Area, Biodonostia Health Research Insitute, San Sebastian, Gipuzkoa, Spain
Caroline Graff	Department of Geriatric Medicine, Karolinska University Hospital-Huddinge, Stockholm, Sweden
Caroline Greaves	Dementia Research Centre, Department of Neurodegenerative Disease, UCL Institute of Neurology, Queen Square, London, UK
Rita Guerreiro	Dementia Research Institute, Department of Neurodegenerative Disease, UCL Institute of Neurology, Queen Square, London, UK
Carolin Heller	Dementia Research Centre, Department of Neurodegenerative Disease, UCL Institute of Neurology, Queen Square, London, UK
Tobias Hoegen	Neurologische Klinik, Ludwig-Maximilians-Universität München, Munich, Germany
Begoña Indakoetxea	Cognitive Disorders Unit, Department of Neurology, Donostia University Hospital, San Sebastian, Gipuzkoa, Spain; Neuroscience Area, Biodonostia Health Research Insitute, San Sebastian, Gipuzkoa, Spain
Vesna Jelic	Division of Clinical Geriatrics, Karolinska Institutet, Stockholm, Sweden
Hans-Otto Karnath	Division of Neuropsychology, Hertie-Institute for Clinical Brain Research and Center of Neurology, University of Tübingen, Tübingen, Germany
Ron Keren	The University Health Network, Toronto Rehabilitation Institute, Toronto, Canada
Robert Laforce	Clinique Interdisciplinaire de Mémoire, Département des Sciences Neurologiques, CHU de Québec, and Faculté de Médecine, Université Laval, Quebec, Canada
Maria João Leitão	Centre of Neurosciences and Cell Biology, Universidade de Coimbra, Coimbra, Portugal
Johannes Levin	Department of Neurology, University Hospital Ulm, Ulm, Germany
Albert Lladó	Alzheimer's disease and Other Cognitive Disorders Unit, Neurology Service, Hospital Clínic, Barcelona, Spain
Sandra Loosli	Neurologische Klinik, Ludwig-Maximilians-Universität München, Munich, Germany
Carolina Maruta	Laboratory of Language Research, Centro de Estudos Egas Moniz, Faculty of Medicine, University of Lisbon, Lisbon, Portugal
Mario Masellis	Sunnybrook Health Sciences Centre, Sunnybrook Research Institute, University of Toronto, Toronto, Canada
Simon Mead	MRC Prion Unit, Department of Neurodegenerative Disease, UCL Institute of Neurology, Queen Square, London, UK
Gabriel Miltenberger	Faculty of Medicine, University of Lisbon, Lisbon, Portugal
Rick van Minkelen	Department of Clinical Genetics, Erasmus Medical Center, Rotterdam, Netherlands
Sara Mitchell	Sunnybrook Health Sciences Centre, Sunnybrook Research Institute, University of Toronto, Toronto, Canada
Katrina Moore	Dementia Research Centre, Department of Neurodegenerative Disease, UCL Institute of Neurology, Queen Square, London UK
Fermin Moreno	Cognitive Disorders Unit, Department of Neurology, Donostia University Hospital, San Sebastian, Gipuzkoa, Spain

Jennifer Nicholas	Department of Medical Statistics, London School of Hygiene and Tropical Medicine, London, UK
Linn Öijerstedt	Department of Geriatric Medicine, Karolinska University Hospital-Huddinge, Stockholm, Sweden
Markus Otto	Istituto di Ricovero e Cura a Carattere Scientifico (IRCCS) Istituto Centro San Giovanni di Dio Fatebenefratelli, Brescia, Italy
Sebastian Ourselin	School of Biomedical Engineering & Imaging Sciences, King's College London, London, UK.
Alessandro Padovani	Centre for Neurodegenerative Disorders, Neurology Unit, Department of Clinical and Experimental Sciences, University of Brescia, Brescia, Italy
Georgia Peakman	Department of Neurodegenerative Disease, UCL Institute of Neurology, UK
Yolande Pijnenburg	Amsterdam University Medical Centre, Amsterdam VUmc, Amsterdam, Netherlands
Cristina Polito	Department of Biomedical, Experimental and Clinical Sciences “Mario Serio”, Nuclear Medicine Unit, University of Florence, Florence, Italy
Sara Prioni	Fondazione IRCCS Istituto Neurologico Carlo Besta, Milano, Italy
Catharina Prix	Neurologische Klinik, Ludwig-Maximilians-Universität München, Munich, Germany
Rosa Rademakers	Department of Neurosciences, Mayo Clinic, Jacksonville, Florida, USA
Veronica Redaelli	Fondazione IRCCS Istituto Neurologico Carlo Besta, Milano, Italy
Tim Rittman	Department of Clinical Neurosciences, University of Cambridge, Cambridge, UK
Ekaterina Rogaeva	Tanz Centre for Research in Neurodegenerative Diseases, University of Toronto, Toronto, Canada
Pedro Rosa-Neto	Translational Neuroimaging Laboratory, McGill Centre for Studies in Aging, McGill University, Montreal, Québec, Canada
Giacomina Rossi	Fondazione IRCCS Istituto Neurologico Carlo Besta, Milano, Italy
Martin Rosser	Dementia Research Centre, Department of Neurodegenerative Disease, UCL Institute of Neurology, Queen Square, London, UK
James Rowe	Department of Clinical Neurosciences, University of Cambridge, Cambridge, UK
Isabel Santana	Neurology Department, Centro Hospitalar e Universitário de Coimbra, Coimbra, Portugal
Beatriz Santiago	Neurology Department, Centro Hospitalar e Universitario de Coimbra, Coimbra, Portugal
Elio Scarpini	Fondazione IRCCS Ca’ Granda Ospedale Maggiore Policlinico, Neurodegenerative Diseases Unit, Milan, Italy; University of Milan, Centro Dino Ferrari, Milan, Italy
Sonja Schönecker	Neurologische Klinik, Ludwig-Maximilians-Universität München, Munich, Germany
Elisa Semler	Department of Neurology, University of Ulm, Ulm
Rachelle Shafei	Dementia Research Centre, Department of Neurodegenerative Disease, UCL Institute of Neurology, Queen Square, London, UK
Christen Shoesmith	Department of Clinical Neurological Sciences, University of Western Ontario, London, Ontario, Canada
Matthis Synofzik	Department of Neurodegenerative Diseases, Hertie-Institute for Clinical Brain Research and Center of Neurology, University of Tübingen, Tübingen, Germany

Miguel Tábuas-Pereira	Neurology Department, Centro Hospitalar e Universitario de Coimbra, Coimbra, Portugal
Fabrizio Tagliavini	Fondazione Istituto di Ricovero e Cura a Carattere Scientifico Istituto Neurologico Carlo Besta, Milan, Italy
Carmela Tartaglia	Tanz Centre for Research in Neurodegenerative Diseases, University of Toronto, Toronto, Canada
Mikel Tainta	Neuroscience Area, Biodonostia Health Research Insitute, San Sebastian, Gipuzkoa, Spain
Ricardo Taipa	Neuropathology Unit and Department of Neurology, Centro Hospitalar do Porto - Hospital de Santo António, Oporto, Portugal
David Tang-Wai	The University Health Network, Krembil Research Institute, Toronto, Canada
David L Thomas	Neuroimaging Analysis Centre, Department of Brain Repair and Rehabilitation, UCL Institute of Neurology, Queen Square, London, UK
Hakan Thonberg	Center for Alzheimer Research, Division of Neurogeriatrics, Karolinska Institutet, Stockholm, Sweden
Carolyn Timberlake	Department of Clinical Neurosciences, University of Cambridge, Cambridge, UK
Pietro Tiraboschi	Fondazione IRCCS Istituto Neurologico Carlo Besta, Milano, Italy
Emily Todd	Department of Neurodegenerative Disease, UCL Institute of Neurology, UK
Philip Vandamme	Neurology Service, University Hospitals Leuven, Belgium; Laboratory for Neurobiology, VIB-KU Leuven Centre for Brain Research, Leuven, Belgium
Rik Vandenberghe	Laboratory for Cognitive Neurology, Department of Neurosciences, KU Leuven, Leuven, Belgium
Mathieu Vandenbulcke	Geriatric Psychiatry Service, University Hospitals Leuven, Belgium; Neuropsychiatry, Department of Neurosciences, KU Leuven, Leuven, Belgium
Michele Veldsman	Nuffield Department of Clinical Neurosciences, Medical Sciences Division, University of Oxford, Oxford, UK
Ana Verdelho	Department of Neurosciences and Mental Health, Centro Hospitalar Lisboa Norte - Hospital de Santa Maria & Faculty of Medicine, University of Lisbon, Lisbon, Portugal
Jorge Villanua	OSATEK, University of Donostia, San Sebastian, Gipuzkoa, Spain
Jason Warren	Dementia Research Centre, Department of Neurodegenerative Disease, UCL Institute of Neurology, Queen Square, London, UK
Carlo Wilke	Department of Neurodegenerative Diseases, Hertie-Institute for Clinical Brain Research and Center of Neurology, University of Tübingen, Tübingen, Germany; Center for Neurodegenerative Diseases (DZNE), Tübingen, Germany
Ione Woollacott	Dementia Research Centre, Department of Neurodegenerative Disease, UCL Institute of Neurology, Queen Square, London, UK
Elisabeth Wlasich	Neurologische Klinik, Ludwig-Maximilians-Universität München, Munich, Germany
Henrik Zetterberg	Dementia Research Institute, Department of Neurodegenerative Disease, UCL Institute of Neurology, Queen Square, London, UK
Miren Zulaica	Neuroscience Area, Biodonostia Health Research Insitute, San Sebastian, Gipuzkoa, Spain